Electronic Supplementary Material (ESI) for ChemComm.
This journal is © The Royal Society of Chemistry 2019

Supporting Information

Role of well-defined cobalt crystal facets in Fischer-Tropsch Synthesis: a combination of experimental and theoretical study

Lei Nie,*[‡a] Zhe Li,[‡a] Ting Kuang,[‡a] Shuai Lyu,[a] Sixu Liu,[a] Yuhua Zhang,[a] Bo Peng,[b] Jinlin Li,[a] Li Wang*[a]

[a]Key Laboratory of Catalysis and Materials Science of the State Ethnic Affairs Commission & Ministry of Education, College of Chemistry and Materials Science, South-Central University for Nationalities, Wuhan 430074, China.

[b] Institute for Integrated Catalysis, Pacific Northwest National Laboratory, 902 Battelle Boulevard, P. O. Box 999, Richland, WA 99352, USA.

‡ These authors contributed equally to this work.

* Corresponding authors:

L.Nie: lei.nie@scuec.edu.cn;

L. Wang: li.wang@scuec.edu.cn; Tel: +86 27 67842922

Experimental

1. Preparation of the catalysts

Preparation of carbon spheres (CSs). Carbon spheres were synthesized by hydrothermal method. 60g glucose was dissolved in 250 mL of deionized water and ultrasonicated for 30min. The obtained solution was transferred into a 500 ml of teflon-lined autoclave, and 100 mL of deionized water was added into the autoclave. The mixture was then kept at 180℃for 10 h. After that, the mixture was adequately washed with ethanol and deionized water until the filter water was clear. Finally the obtained precipitate was dried at 100℃ for 12 h followed by calcination at 800 ℃ in N_2 for 2 h in a tube furnace. The obtained black power was denoted as carbon spheres (CSs).

Preparation of hcp-CoO pyramid. A black slurry of $Co(acac)_3$ (0.5 g), CSs (0.5 g) and benzylamine (30.0 g) were added to a 250 mL three-necked flask connected to a water condenser for cycling the evaporated benzylamine back to the flask. The mixture was vigorously stirred in a preheated oil bath at 200 ℃ for 1 h, and cooled to room temperature. Afterwards the mixture was washed three times with ethanol then dried at 100 ℃ for 10 h. The obtained black power was denoted as hcp-CoO pyramid.

Preparation of hcp-CoOrodlike. A black slurry of $Co(acac)_3$ (0.5 g), CSs (0.5 g), benzylamine (30.0 g) and o-dichlorobenzene (15 g) was heated to 135 ℃ and kept for 30 min. Then the mixture was refluxed in a preheated oil bath at 185 ℃ for 1 h. After being cooled to room temperature, the mixture was washed three times with ethanol and dried at 100 ℃ for 10 h. The obtained black power was denoted as hcp-CoOrodlike.

Preparation of fcc-CoO octahedral. A black slurry of $Co(acac)_3$ (0.3 g), CSs (1.0 g)

and benzylamine (30.0 g) was vigorously stirred and heated to 175 ℃. The mixture was kept at 175 ℃ for 1 h and cooled to room temperature. Then the mixture was washed three times with ethanol and dried at 100 ℃ for 10 h. The obtained black power was denoted as fcc-CoO octahedral.

Preparation of metallic Co catalysts. The above CoO catalysts were reduced in-situ 10% H_2/90%Ar (3 SL h^{-1} g^{-1}) at 623 K for 3h before FTS reaction. The obtained catalysts were denoted as hcp-Co pyramid, hcp-Co rodlike and fcc-Co octahedral.

2. Characterizations

The composition and phase of the samples were identified by X-ray powder diffraction (XRD) (Bruker D8 Advance) with monochromated Cu Kα radiation operated at 40 kV and 40 mA and a Vantec-1 detector. The size and morphology of samples were determined using a FEI Tecnai G20 transmission electron microscope (TEM) operated at 200 kV and SU8000 field emission scanning electron microscope (FESEM, Hitachi, Japan) at anaccelerating voltage of 15 kV. The CO adsorption performance of samples was measured by in-situ diffuse reflectance FTIR spectroscopy (in-situ DRIFTS) (Nicolet NEXUS 6700). The number of surface active metal atoms was measured by hydrogen chemisorption (H_2-TPD) (Micromeritics AutoChem II 2920 unit).

Under low conversion (< 10 %), turnover frequency (TOF) was calculated as follows:

$$TOF\left(s^{-1}\right) = \frac{S \cdot R \cdot X}{3600 \cdot 22.4 \cdot D}$$

Here S represents GHSV [L (g_{cat} h)$^{-1}$], R represents CO fraction in gas feed, X represents CO conversion (%), and D represents the concentration of surface active site derived from H_2 chemisorption measurements [mol g_{cat}^{-1}].

3. Catalytic test

The Fischer-Tropsch synthesis was performed in a stainless-steel tube fixed-bed

reactor. 0.2 g catalyst was added into the reactor and reduced in-situ 10% H_2/90%Ar (3 SL h^{-1} g^{-1}) at 623 K for 3h. After reduction, the catalyst was cooled to 373 K in flowing 10% H_2/90%Ar. Then, the syngas ($H_2/CO/N_2$ = 6/3/1) was introduced. The space velocity of syngas was 1 SL h^{-1} g^{-1}. The pressure was increased to 1 MPa, and the reaction temperature slowly increased to the specified temperature. The effluent gas from the fixed bed reactor was analyzed online using gas chromatograph (GC) (Agilent 7890B), equipped with one thermal conductivity detector (TCD) and two flame ionization detectors (FIDs).The product selectivity was calculated based on the carbon mass balance. The calculated carbon balance is ~ about 95.0 % and the mass balance is> 94.0 %.

The conversion of CO and selectivity of hydrocarbon (carbon number based) were calculated as below.

CO conversion: $$X\,(\%) = \frac{CO\,(in) - CO\,(out)}{CO\,(in)} \times 100\%$$

CH4 selectivity: $$S_{methane}\,(\%) = \frac{CH_4}{CO\,(in) - CO\,(out) - CO_2\,(out)} \times 100\%$$

Cn selectivity (n = 2, 3 and 4): $$S_n\,(\%) = \frac{n \times C_n}{CO\,(in) - CO\,(out) - CO_2\,(out)} \times 100\%$$

C_5^+ selectivity: $$S_{5+}\,(\%) = \left(1 - S_{methane} - S_2 - S_3 - S_4\right) \times 100\%$$

CO_2 selectivity: $$S_{CO_2}\,(\%) = \frac{CO_2\,(out)}{CO\,(in) - CO\,(out)} \times 100\%$$

Under low conversion (< 20%), turnover frequency (TOF) was calculated as below.

$$TOF\left(s^{-1}\right) = \frac{S \cdot R \cdot X}{3600 \cdot 22.4 \cdot D}$$

Here S represents GHSV [L (g_{cat} $h)^{-1}$], R represents CO fraction in gas feed, X represents CO conversion (%) and D represents the concentration of the surface active site derived from H_2 chemisorption measurements [mol g_{cat}^{-1}].

4. Computational details

Density functional theory calculations were performed using PBE functional[1] and projector-augmented wave (PAW) method[2] as implemented in Vienna ab initio simulation package (VASP).[2, 3] Second-order Methfessel-Paxton smearing scheme (sigma = 0.2 eV) was used for modeling the metal systems. Spin polarization effects was considered using plane wave energy cutoff of 400 eV. Different Monkhorst-Pack *k*-point schemes, i.e., 3 × 5 × 1, 5 × 3 × 1, and 5 × 5 × 1, were used for the 4-layered hcp-Co(10-11), hcp-Co(10-10) and fcc-Co(111) slab surfaces in *p*(2 × 2) supercells, respectively. A vacuum of 15 Å was added to separate the repeated slab models in the normal direction. The top two layers and the adsorbates were allowed to relax with energy (10^{-5} eV) and force convergences (0.03 eV/Å) while the bottom two layers were kept fixed. We use quasi-Newton algorithm (IBRION=1) for the optimization of transition states, some of which are confirmed by climbing image nudge-elastic band (CI-NEB) method. The optimized structures were determined to be local minima or transition states on the potential energy surfaces by frequency calculations without or with no more than one imaginary frequency. The reaction pathways were initiated from the most stable adsorption of the reactants and terminated by the most stable geometries of the products. The transfer kinetics of the intermediate species on the Co surface was not considered.

Based on harmonic transition-state theory, the rate constant *k* can be calculated by

$$k = \mathrm{A}\exp\left(-\frac{E_a}{RT}\right)$$

$$= \frac{k_B T q^{TS}}{h \quad q^{IS}} \exp\left(-\frac{E_0}{RT}\right)$$

in which *A* is the pre-exponential factor

$$A = \frac{k_B T q^{TS}}{h \quad q^{IS}}$$

E_a is activation energy; E_0 is the ZPE-corrected total energy difference between the transition state (TS) and initial state (IS)

$$E_0 = E_a + \Delta ZPE$$

$$\Delta ZPE = ZPE^{TS} - ZPE^{IS}$$

$$ZPE = \sum_{i}^{3N} \frac{hv_i}{2}$$

q is vibrational partition function of surface species.

$$q = \sum_{i}^{3N} \frac{1}{1 - e^{-hv_i/k_B T}}$$

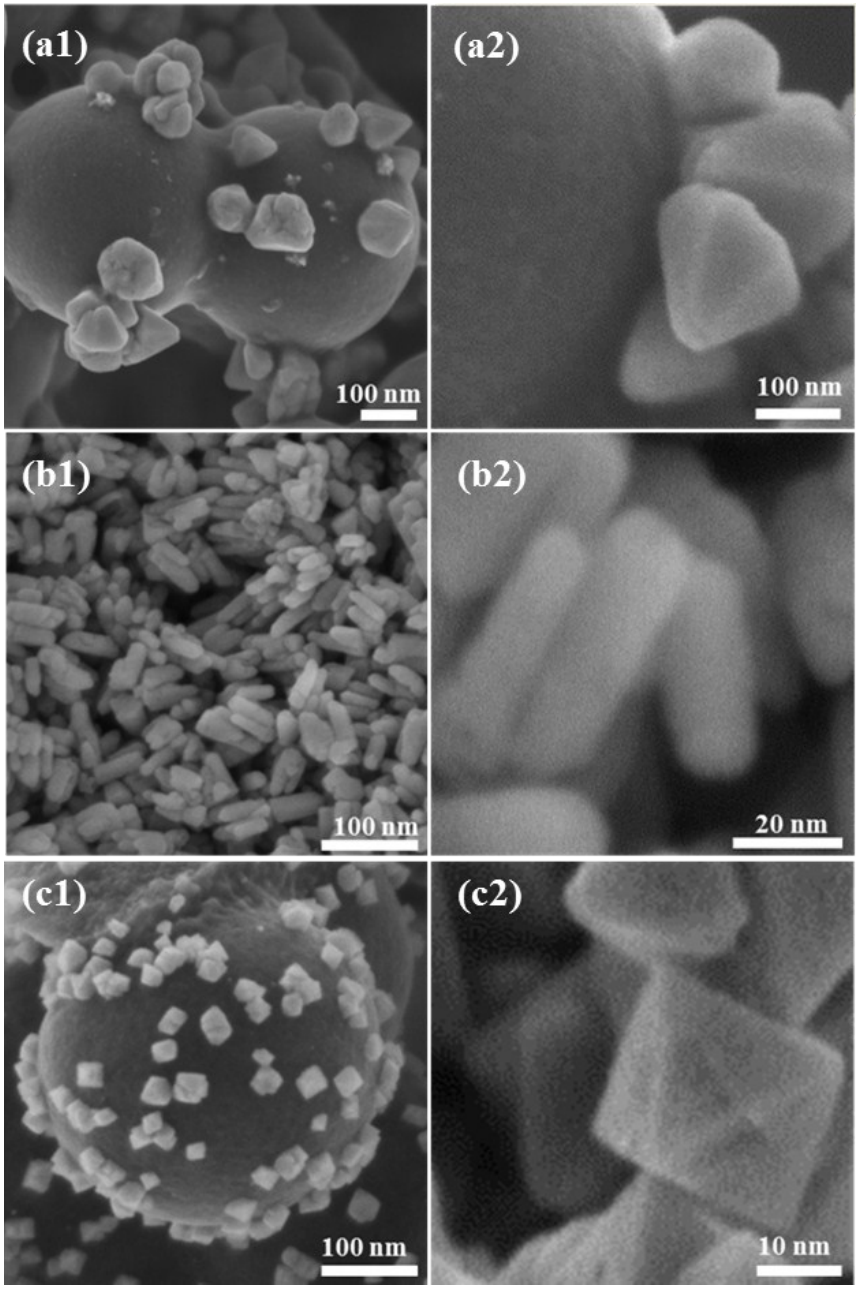

Figure S1. Electron microscopic characterization of CoO nanocrystals. (a1, a2) hcp-CoO pyramid, (b1, b2) hcp-CoO rodlike and (c1, c2) fcc-CoO octahedral.

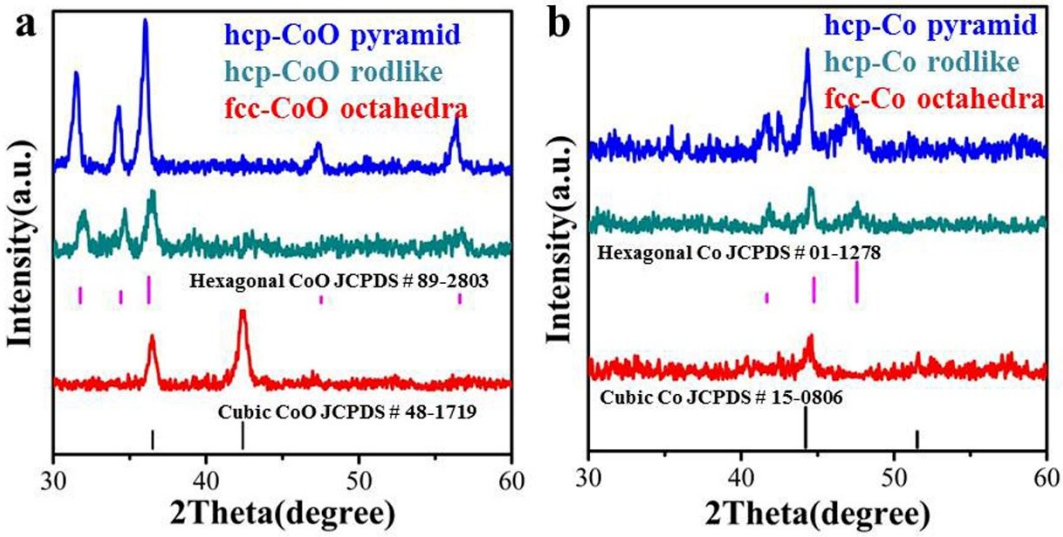

Figure S2. (a) XRD patterns of CoO nanocrystals with different shapes. (b) XRD patterns of the corresponding Co catalysts. hcp-Co pyramid (blue line), hcp-Co rodlike (aqua line) and fcc-Co octahedral (red line).

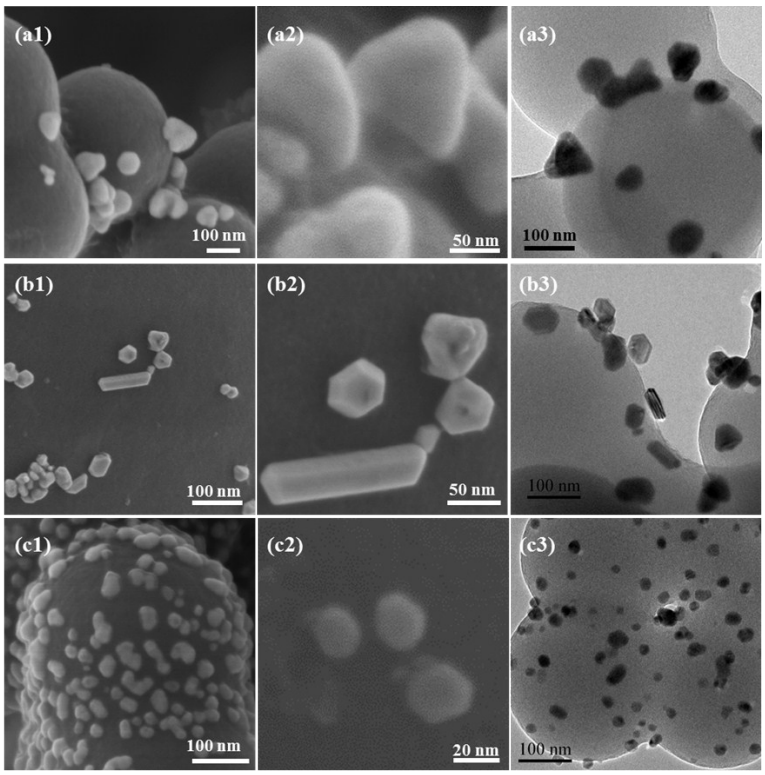

Figure S3. Electron microscopic characterizations of the spent catalysts. (a1-c1, a2-c2) SEM images. (a3-c3) TEM images. (a1-a3) hcp-Co pyramid, (b1-b3) hcp-Co rodlike, (c1-c3) fcc-Co octahedral.

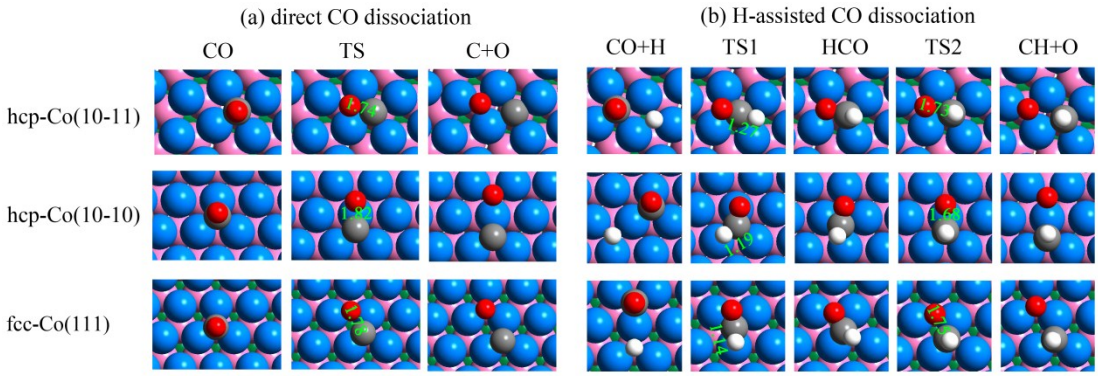

Figure S4. Optimized geometries for CO dissociations on hcp-Co(10-11), hcp-Co(10-10) and fcc-Co(111) surfaces indicated by the C-O and C-H bond distances (in Å) in the TS structures (TS: transition state; C: grey; H:white; O: red; Co-top-layer: blue; Co-sub-layer: pink; Co-3rd-layer: green).

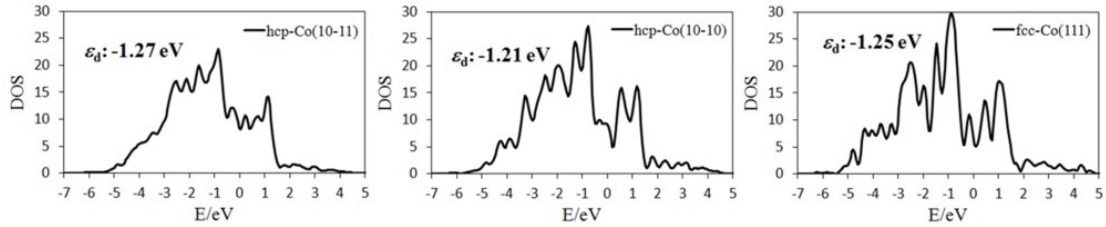

Figure S5. Density of state (DOS) of Co-3d on hcp-Co(10-11), hcp-Co(10-10) and fcc-Co(111) surfaces indicated the d-band center (ε_d).

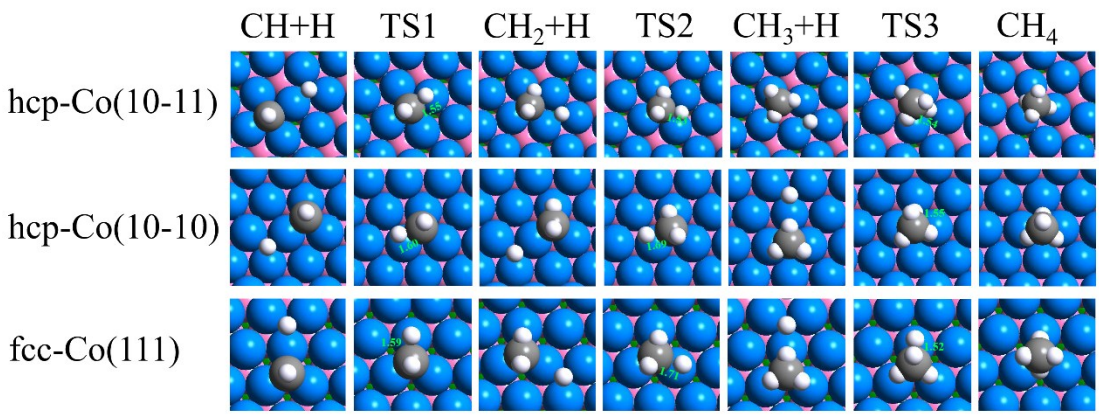

Figure S6. Optimized geometries for CHx (x = 1-3) methanation reactions on hcp-Co(10-11), hcp-Co(10-10) and fcc-Co(111) surfaces indicated by the C-H bond distances (in Å) in the TS structures (TS: transition state; C: grey; H:white; Co-top-layer: blue; Co-sub-layer: pink; Co-3rd-layer: green).

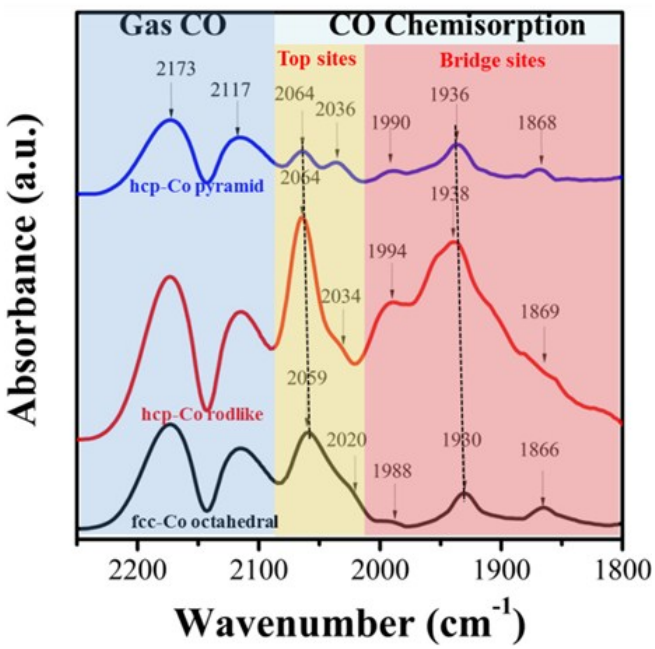

Figure S7. In-situ DRIFTS spectra of CO adsorption on the reduced Co catalysts at 40 °C in high purity syngas 60% H_2 /30 % CO / 10% N_2. hcp-Co pyramid (blue line), hcp-Co rodlike (red line), fcc-Co octahedral (black line).

Table S1. H_2 chemisorption, Co content and Co particle size results for the Co-based catalysts

Catalyst	H_2 uptake (μmol g^{-1})[a]	Co Content (wt.%)[b]	d_{Co} (nm)[c]
hcp-Co-p	26.3	8.5	70.9
hcp-Co-r	38.8	7.2	41.2×14.0
fcc-Co-o	51.6	5.2	24.9

[a] H_2 chemisorption performance at the procedure of sample (0.05 g) reduced in situ at 370 °C for 3 h in a flow (25 mL min^{-1}) of H_2, then the temperature was increased from 50 to 450 °C and kept for 30 min after the temperature decreasing in a flow (25 mL min^{-1}) of Ar.

[b] Co content was determined by ICP analysis.

[c] Co particle size was obtained by SEM analysis.

Table S2. DFT-calculated energy barrier (E_a) for CO dissociation compared with the results in literatures

E_a (eV)	hcp-Co(10-11)		hcp-Co(10-10)		fcc-Co(111)	
	direct	H-assist	direct	H-assist	direct	H-assist
Our DFT	1.09	1.37	1.75	1.54	2.40	1.87
Ref. DFT[a]	1.21	1.44	1.79	1.50	2.48	1.84
FTS exp.	0.77		0.91		1.21	

[a] Referenced are data from literatures 4-6.

Table S3. Calculated kinetic parameters for the CO dissociations at 473 K.

surface	q^{IS}	q^{TS}	E_0/eV	A/s^{-1}	k/s^{-1}
hcp-Co(10-11)	51.65	5.69	1.06	1.09×10^{12}	6.29
hcp-Co(10-10)[a]	113.52	14.59	1.58	1.27×10^{12}	2.06×10^{-5}
fcc-Co(111)[a]	99.50	12.23	1.93	1.21×10^{12}	3.53×10^{-9}

[a] The rate-determining energy barrier ($E_{TS2} - E_{IS}$) is used for the H-assisted CO dissociation.

Table S4. Bader charges of cobalt surfaces in the transition state structures of the direct and H-assisted CO dissociations

Bader charge (|e|)	Direct dissociation	H-assisted dissociation
	TS1	TS2
hcp-Co(10-11)	1.34	1.11
hcp-Co(10-10)	1.23	1.07
fcc-Co(111)	1.09	0.99

References

1. Perdew, J. P.; Burke, K.; Ernzerhof, M., *Phys. Rev. Lett.* **1996**, *77*, 3865.
2. Kresse, G.; Joubert, D., *Phys. Rev. B* **1999**, 59,1758-1775.
3. Kresse, G.; Furthmüller, J., *Phys. Rev. B: Condens. Matter Mater. Phys.* **1996**, *54*, 11169.
4. Liu J.-X.; Su H.-Y.; Sun D.-P.; Zhang B.-Y.; Li W.-X., *J. Am. Chem. Soc.,* 2013, **135**, 16284-16287.
5. Zhang R.; Li K.; Liu H.; He L.; Wang B., *Comput. Mater. Sci.* 2018, **145**, 263-279.
6. Chen C.; Wang Q.; Wang G.; Hou B.; Jia L.; Li D., *J. Phys. Chem. C* 2016, **120**, 9132-9147.